

Revolutionizing Access Networks: How TFDM Coherent PON Combines the Best of TDM and WDM PONs

A Technical Paper prepared for SCTE by

Zhensheng (Steve) Jia, Ph.D.

Fellow and Director of Advanced Optical Technologies
CableLabs
858 Coal Creek Circle, Louisville CO, 80027
303.661.3364
s.jia@cablelabs.com

Haipeng Zhang, Ph.D.

Lead Architect
CableLabs
858 Coal Creek Circle, Louisville CO, 80027
303.661.3796
h.zhang@cablelabs.com

L. Alberto Campos, Ph.D.

Fellow
CableLabs
858 Coal Creek Circle, Louisville CO, 80027
303.661.3377
a.campos@cablelabs.com

Table of Contents

Title	Page Number
1. Introduction and Motivation	4
1.1. PON Evolution.....	4
1.2. Coherent Optics Technology Evolution.....	5
1.3. Coherent PON.....	6
1.4. Coherent TDM-PON and Coherent WDM-PON.....	7
1.5. Coherent TWDM-PON and Coherent TFDM-PON	8
2. TFDM CPON Technology and Architecture Overview.....	10
3. TFDM CPON Key Technology Development.....	11
3.1. Burst Signal Processing in TFDM Subcarriers.....	12
3.2. Subcarrier Recognition, Pre-equalization, and Power Rebalancing	15
3.3. ONU Cost Reduction Through Remote Optical Carrier Delivery	19
4. Advantages, Challenges, and Discussions	23
5. Conclusions.....	25
6. Acknowledgements	25
Abbreviations	26
Bibliography & References.....	27

List of Figures

Title	Page Number
Figure 1 – Standardized PON Evolution	4
Figure 2 – The Next Application Fields for Coherent Optics.....	6
Figure 3 – CPON Supporting Various Applications	7
Figure 4 – Examples of PON Architecture: (a) Time-Division Multiplexing (TDM); (b) Wavelength-Division Multiplexing (WDM)	8
Figure 5 – Examples of PON Architecture: (a) Time and Wavelength Division Multiplexing (TWDM); (b) Time and Frequency Division Multiplexing (TFDM).....	9
Figure 6 – Principle of TFDM CPON based on digital subcarrier multiplexing scheme: (a) architecture; (b) example of flexible data/bandwidth allocation	10
Figure 7 – TFDM DSP flow: (a) Tx subcarrier generation DSP; (b) Rx subcarrier demodulation DSP.....	11
Figure 8 – (a) TFDM burst Tx DSP procedures; (b) TFDM burst Rx DSP procedures; (c) Preamble design in TFDM burst frame.....	13
Figure 9 – TFDM burst optimization and performance evaluation: (a) Double-Correlation pattern in TFDM burst operation under different synchronization symbol length; (b) TDM burst BER performance under residual CD; (c) TDM burst BER performance under CFO	14
Figure 10 – Proposed DSP procedures featuring subcarrier recognition, pre-equalization, and power rebalancing in: (a) TFDM coherent burst receiver; (b) TFDM coherent transmitter.....	16
Figure 11 – Process of CR-FC, Pre-EQ, and PR of TFDM signal	17
Figure 12 – CR-FC algorithm performance: (a) channel boundary detection with large CFO; (b) BER versus frequency detuning using different methods	18
Figure 13 – (a) BER performance with and without Pre-EQ + PR; (b) BER performance	18
Figure 14 – (a) TFDM CPON scheme with remote optical tone delivery; (b) subchannel design for DS and US transmission	19

Figure 15 – (a) Experimental setup with optical spectrums of TFDM DS and US channels; (b) BER versus ROP in downstream; (c) BER versus ROP in upstream 21

Figure 16 – (a) Residual CFO for proposed OIL scheme vs. regular ECL-based system; (b) BER vs. ROP per channel for proposed OIL scheme without CFO correction compared with regular ECL-based system with CFO correction 22

Figure 17 – Technical summary of DSC based TFDM CPON..... 23

1. Introduction and Motivation

The modern world heavily depends on the swift and dependable sharing of information. The growing need for faster data speeds and greater network capacity consistently surpasses the capabilities of existing systems [1, 2]. Passive optical networks (PONs) have experienced significant advancements in the last twenty years and are now considered highly appealing as access network solutions for providing high-speed data and video services [3, 4]. A PON is an economical and efficient optical communication network technology that uses fiber optics to deliver various broadband services to users. PON architecture adopts a point-to-multipoint (P2MP) structure and employs passive optical components to establish connections between service providers and customers. Passive fiber optic splitters play a crucial role in PON architecture as they divide the signal in a way that each port receives the same data signal, although depending on the splitter design, different ports may have varying power levels. To meet the increasing bandwidth demand driven by data intensive applications such as video streaming, 5G mobile Internet, and cloud networking, several generations of PON systems have been standardized through the efforts of two major organizations: the International Telecommunication Union Telecommunication Standardization Sector (ITU-T) and the IEEE 802.3 Ethernet Working Group, as shown in Figure 1.

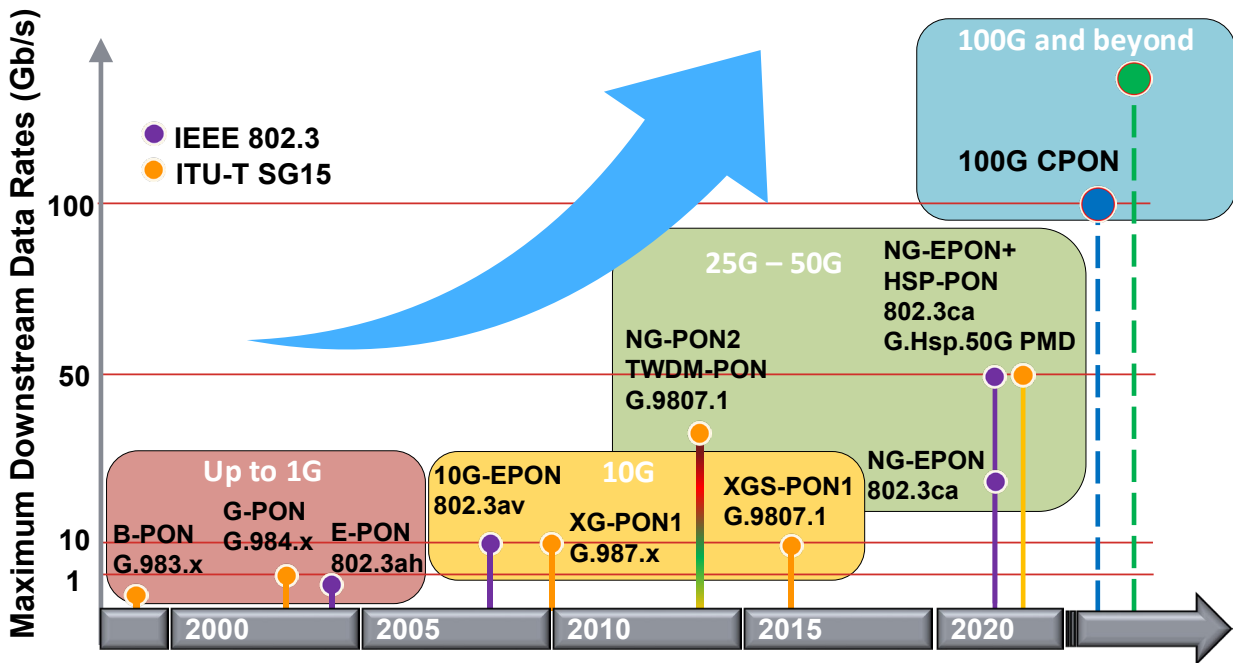


Figure 1 – Standardized PON Evolution

1.1. PON Evolution

The initial standardized PONs, namely asynchronous transfer mode PON (APON) and broadband PON (BPON) defined in G.983, were introduced by the ITU-T in the late 1990s. These systems offered a symmetric line rate ranging from 155 Mb/s to 622.08 Mb/s. Following this, the widely deployed gigabit PON (GPON) defined in G.984 was standardized in 2003, offering downstream speeds of up to 2.5 Gb/s. It had a maximum reach of 20 km and a maximum split ratio of 1:64. The IEEE standardized the Ethernet PON (EPON) as 802.3ah in 2004. EPON utilized ethernet frames and provided a symmetric line rate of 1.25 Gb/s, with a maximum reach of 20 km and a split ratio of 1:32. In 2009, the 10G EPON standard (802.3av) was released, offering a symmetrical line rate of 10.3125 Gb/s. The ITU-T introduced the next-

generation PON (XG PON) in 2010 (G.987), providing downstream speeds of 10 Gb/s and upstream speeds of 2.5 Gb/s. The next-generation PON stage 2 (NG-PON2) was standardized in 2015 (G.989), utilizing time- and wavelength- division multiplexing (TWDM) architecture to support 4-8 wavelengths with a broadband speed of 10 Gb/s per wavelength. The next-generation symmetric PON (XGS PON), a symmetric version of XG PON, offered a symmetrical line rate of 10 Gb/s for both downstream and upstream. Recently, the IEEE 802.3ca Nx25G EPON Task Force defined a system based on a 25 Gb/s line rate, aiming to standardize a 100G-EPON initially but scaled back to a 2x25 Gb/s system [5]. On the ITU-T side, in 2021, a suite of G.9804 Recommendations (G.hsp) was developed, focusing on a 50 Gb/s line rate PON system to lay the groundwork for future ITU-T PON systems [6]. The Common Transmission Convergence (ComTC) layer in G.9804.2 is designed to be agnostic of transmission rates, wavelength channels, and signal modulation, making it applicable to future time-division-multiplexing (TDM) and TWDM PON systems.

The current PONs utilize intensity modulation–direct detection (IM-DD) technology to achieve a cost-effective and efficient balance. By prediction, PON technology of 100 Gb/s per wavelength and beyond is expected to be required soon to meet the ever-increasing demands for higher capacities. Lately, Nokia has demonstrated 100 Gb/s PON based on IM/DD pulse amplitude modulation 4-level (PAM-4) and flexible forward error correction (FEC) code rate [7]. However, as PON development progresses, certain factors come into play. These factors include the need for increased launched power, improved forward error correction (FEC), and higher sensitivity receivers to meet around 29-dB loss budget and optical path penalty required for higher data rates. This power budget is essential to ensure compatibility with existing PON infrastructure, as deploying fiber networks entails significant investment. Nonetheless, this trend changes when data rates exceed 25 Gb/s, as IM-DD technology faces physical challenges that result in higher costs and power consumption for the overall system architecture and optical design. To tackle these challenges, several requirements and considerations emerge. These include the need for high sampling rate digital-to-analog converters (DAC) and analog-to-digital converters (ADC) to enable signal processing in the digital domain. Additionally, digital signal processing algorithms play a vital role in compensating for device bandwidth limitations and mitigating transmission impairments. Due to limited link budgets, optical amplification becomes necessary in both centralized optics and customer premise equipment. The congestion in the O-band for both downstream and upstream adds complexity to wavelength planning and resource management. Furthermore, the utilization of higher bandwidth optoelectronic components becomes imperative to minimize implementation penalties. Hence, when aiming for data rates reaching and exceeding 100 Gb/s on a single wavelength, the utilization of IM-DD technology becomes considerably difficult.

1.2. Coherent Optics Technology Evolution

On the other hand, the introduction of coherent optical technology has had a profound impact on optical transmission systems, leading to extensive upgrades and the implementation of dense wavelength division multiplexing (DWDM) networks operating at speeds of 100 Gbps, 200 Gbps, and 400 Gbps per wavelength. Initially developed for long-haul applications, coherent optics has evolved and is now being widely employed in metro networks. This transition has been facilitated by advancements in complementary metal-oxide semiconductor (CMOS) manufacturing, simplified design approaches, cost reduction in optoelectronic components, and the demand for more efficient optical transport technologies. As a result, coherent solutions are now being integrated into new market segments, particularly for short-haul applications in edge and access networks. This progression from long-distance to short-distance models has been observed previously in the optical industry, as DWDM technology initially emerged in long-haul scenarios before being adopted in metro and edge access networks.

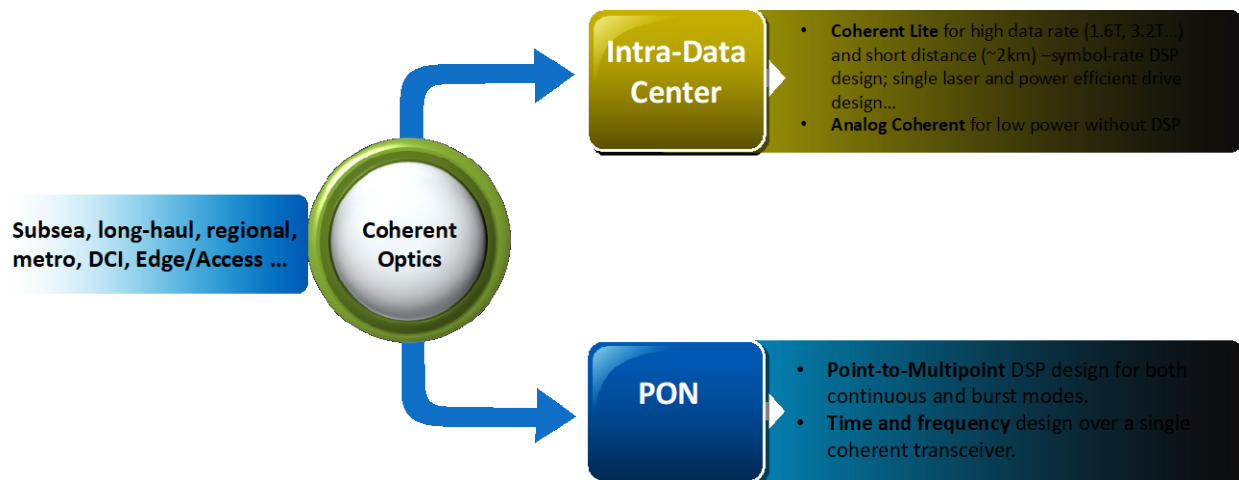


Figure 2 – The Next Application Fields for Coherent Optics

Building upon the foundation laid by long-haul technology development, coherent optics is set to follow a similar natural progression into access networks as shown in Figure 2. The forthcoming horizons of coherent optical networking are anticipated to encompass intra-data center communication and point-to-multipoint PONs. Progress has been made in the advancement of power-efficient designs targeting intra-data center application through the utilization of coherent lite, analog coherent, and mixed-domain coherent technologies. These innovations hold the promise of achieving data transmission rates of up to 3.2Tb/s over distances of less than 2 km within intra-data center environments, all while maintaining comparable advantages with conventional IM-DD systems in terms of cost, power efficiency, and latency. On the other hand, the inception of CableLabs’ Coherent PON (CPON) project, initiated two years ago, is emblematic of a collective endeavor aimed at realizing the next-generation 100G point-to-multipoint access architecture.

1.3. Coherent PON

CPON is the application of coherent optical transmission principles to PON technology, offering numerous advantages for access networks. CPON utilizes multiplexing in multiple dimensions (optical amplitude, phase, and polarization) to encode information, enabling higher data rates with low-bandwidth analog and digital signal processing techniques. By employing a local oscillator, CPON achieves significant coherent gain, resulting in superior receiver sensitivity and a high-power budget without the need for excessive launched power. The recovered signal facilitates digital compensation of linear transmission impairments, such as chromatic dispersion (CD) and polarization-mode dispersion (PMD), with minimal optical path penalty, enabling the implementation of ultra-long reach PON.

CPON technology sets itself apart from IM-DD technology by providing several benefits for network operators. These include expanded use cases and coverage areas through higher link budgets, the potential for cost reduction by scaling back or eliminating expensive facilities for distant communities, the ability to increase subscriber counts without a linear increase in fiber usage through wavelength stacking in the C-band, and the flexibility to support convergence needs for optical signal transport functions at the network edge, extending PON's applications beyond traditional residential deployments.

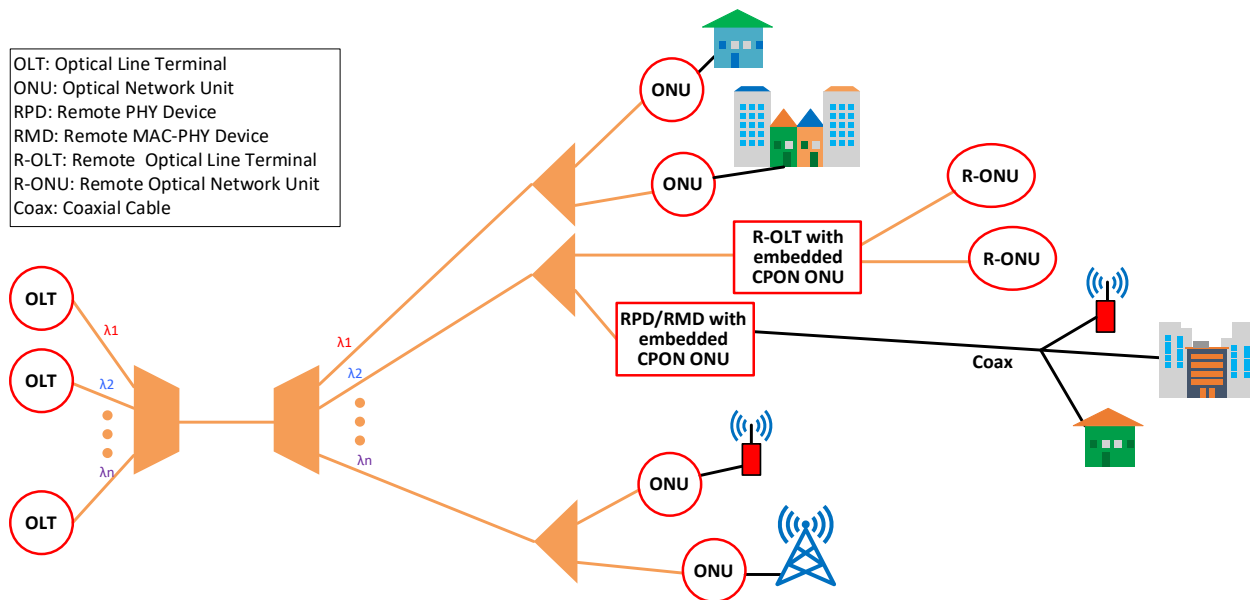


Figure 3 – CPON Supporting Various Applications

In addition to fiber to the home (FTTH) covering multiple dwelling units (MDUs) and single-family units (SFUs), CPON has the capability to support a wide range of applications, as depicted in Figure 3. For instance, CPON can facilitate backhaul connectivity for remote devices within an operator's network, enabling connectivity and backhaul of remote OLT traffic. It can also handle the traffic collected from Remote PHY devices (RPDs) and Remote MAC-PHY devices (RMDs) in a distributed Converged Cable Access Platform (CCAP) architecture. Moreover, CPON can provide mobile backhauling services by offering base station connectivity and carrying mobile backhaul traffic. It is designed to coexist with existing fiber-based technologies like legacy PON systems or wavelength-division multiplexing (WDM) point-to-point links, while also supporting the stacking of multiple CPON wavelengths on a single fiber using WDM. These features greatly enhance deployment flexibility across various scenarios, from high-density interconnects in densely populated urban areas to low-density deployments over rural areas.

1.4. Coherent TDM-PON and Coherent WDM-PON

There have been reports on two types of coherent PON: coherent TDM-PON [8, 9] and coherent WDM-PON [10, 11]. A coherent TDM-PON architecture, as illustrated in Figure 4 (a), is based on a commonly used power splitter-based optical distribution network (ODN). In this architecture, the OLT transmits the downstream signal continuously to each ONU on a single wavelength channel. For upstream transmission, each ONU is allocated a specific timeslot to send a burst of upstream data on another wavelength channel. Alternatively, Figure 4 (b) depicts a coherent WDM-PON architecture where a dedicated wavelength is assigned to each ONU, enabling a virtual point-to-point optical connection. This architecture utilizes a wavelength-routed ODN with inherent wavelength routing capability through wavelength splitters. Coherent WDM-PON and TDM-PON both exhibit significant performance improvements compared to traditional IM-DD PON, thanks to the utilization of coherent detection. On the other hand, although coherent TDM-PON offers a practical approach by efficiently sharing bandwidth in the time domain, it may require a new scheduling algorithm to reduce latency in larger coverage groups. Coherent WDM-PON allows for more flexible allocation of bandwidth but necessitates the use of multiple wavelengths and colored optics, which can result in additional costs and operational complexities.

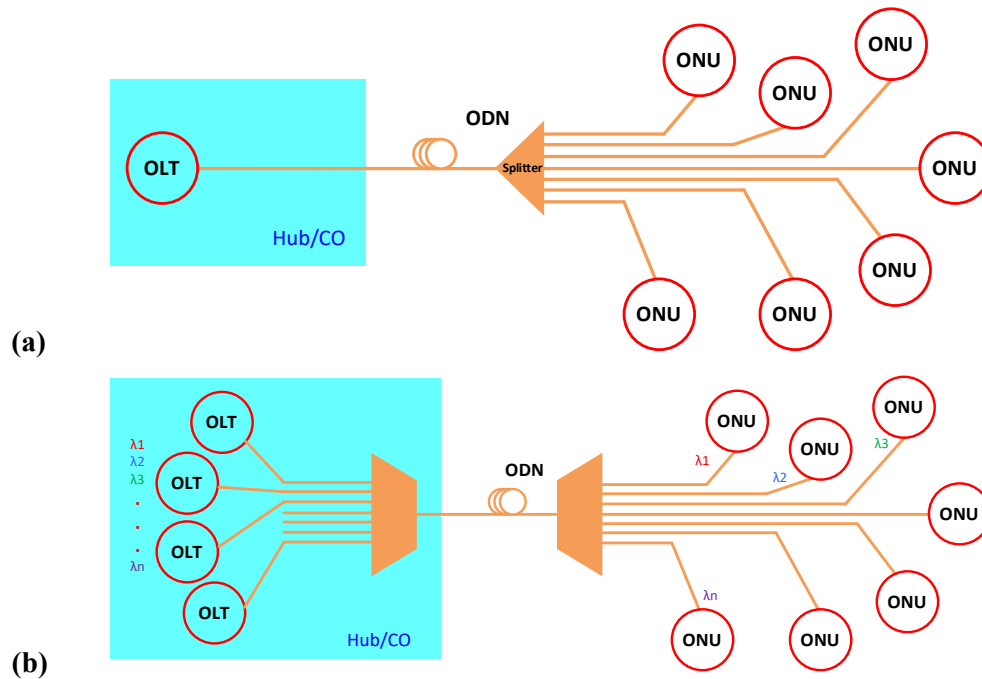


Figure 4 – Examples of PON Architecture: (a) Time-Division Multiplexing (TDM); (b) Wavelength-Division Multiplexing (WDM)

1.5. Coherent TWDM-PON and Coherent TFDM-PON

The next generation access network can benefit from combining the strengths and addressing the limitations of TDM-PON and WDM-PON to achieve more versatile bandwidth allocation. Time and Wavelength Division Multiplexing (TWDM) stands as an alternate form of multiplexed PON architecture harnessed by NG-PON2, enabling multiple signals to be transmitted simultaneously over a single ODN. Coherent technology can be implemented in TWDM-PON, which combines both TDM and WDM technologies mentioned earlier. In TWDM-PON, multiple optical signals are transmitted over the same fiber by assigning different wavelengths to each signal. Each wavelength channel can carry its own independent data stream, and time slots within each channel are used to transmit data from different users or services. Another promising solution for coherent PON is Time and Frequency Division Multiplexing (TFDM), which utilizes digital subcarrier (DSC) multiplexing technology [12-15]., TFDM is a technique that combines TDM and frequency division multiplexing (FDM). In TFDM, multiple optical signals are transmitted over the same fiber by allocating different frequency bands to each signal. Each frequency band can carry its own independent data stream, and time slots within each band are used to transmit data from different users or services. both TWDM and TFDM are techniques that leverage combinations of time, wavelength, and frequency division multiplexing to achieve higher data transmission capacities in PONs as shown in Figure 5. The key difference lies in whether they primarily use wavelength channels (TWDM) or frequency bands (TFDM) to separate data streams. In TWDM architecture, for each wavelength channel, a dedicated transmitter and receiver are necessary for both directions. This involves the use of optical mux/demux and tunable optical filters for effective channelization. The spacing between each wavelength can be as wide as 100GHz or more, allowing for the use of cost-effective optical filtering devices. The commercial reality of NG-PON2 reveals a setup with four channels operating at a

100 GHz spacing. It adopts a 10G/10G TWDM approach, facilitating 10 Gbps upstream and downstream data flow, exclusively tailored for 10G ONUs.

However, in the case of TFDM, frequency division multiplexing occurs in the digital domain, where a single transmitter and receiver can handle any given DSC. The inherent coherent selection filtering capability of TFDM enables its direct application within the power splitter based ODN. This TFDM coherent systems based on the DSC partition data into multiple narrower intermediate digital carriers. These carriers are then modulated onto the optical carrier in a parallel fashion. This technique occupies a comparable bandwidth to single-carrier modulation, utilizing identical modulation formats and total transport capacity. As shown in Figure 5 with four DSCs, while the OLT handles the transmission and reception of all DSCs, individual ONU nodes have the flexibility for modulating and demodulating only a specific subset of these sub-carriers. TFDM CPON offers considerable flexibility by leveraging the sharing of bandwidth in both the time and frequency domains, eliminating the need for colored optics. By employing TFDM DSCs in the frequency domain, different frequency bands can be assigned to network services or groups of ONUs with distinct latency or capacity requirements. This approach can significantly reduce scheduling latency and traffic blocking rates. Furthermore, TFDM technology enables efficient bandwidth granularity and utilization, flexible link budget designs, and scalable architecture. The enhanced flexibility and capability of coherent TFDM technology positions it as a compelling candidate for future access networks.

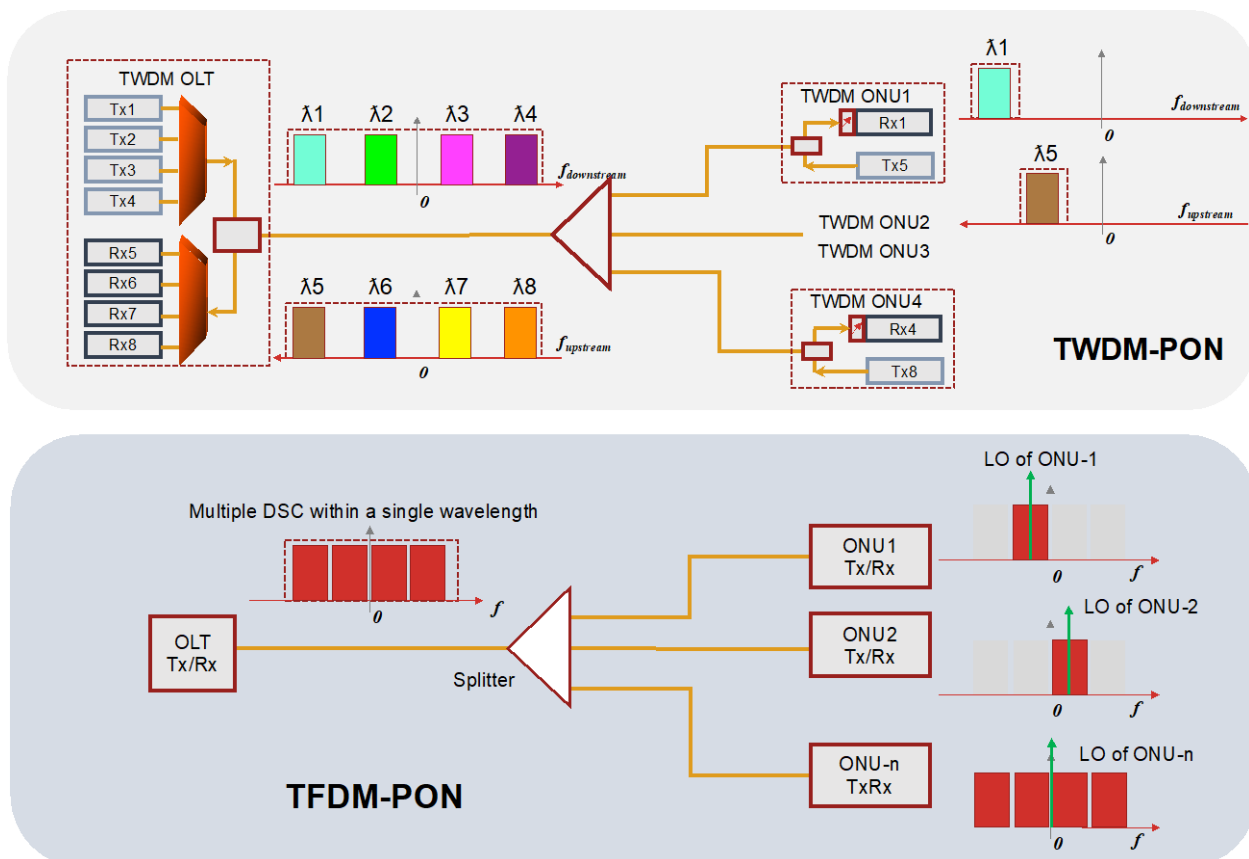


Figure 5 – Examples of PON Architecture: (a) Time and Wavelength Division Multiplexing (TWDM); (b) Time and Frequency Division Multiplexing (TFDM)

2. TFDM CPON Technology and Architecture Overview

Leveraging DSCs in frequency domain and time domain burst processing, TFDM CPON offers unprecedentedly high degree of flexibility in terms of capacity and resource allocation. Figure 6 depicts the structure of a TFDM CPON that utilizes DSC multiplexing technology. In Figure 6 (a), the architecture of a 100G CPON with four subcarriers is presented, as an example. In the downstream direction, the four subcarriers are generated and modulated on a single wavelength in the optical line terminal (OLT) using a coherent I/Q modulator. The coherent receivers in optical network units (ONUs) detect the multi-subcarrier signal downstream and each sub-band can be demodulated individually. In the upstream direction, each ONU can generate and modulate one to four subcarriers, with data rates ranging from 25 Gb/s to 100 Gb/s. Consequently, the aggregated upstream signal comprises four subcarriers, which may originate from the same ONU or different ONUs. Unlike IM/DD technology, which requires multiple receivers and different wavelengths for different subcarriers from different ONUs, TFDM CPON only needs a single broadband coherent receiver at the OLT-side to detect the four subcarriers, even if they come from different ONUs. This represents a significant distinction between the two methods in terms of multiple sub-carrier detection. Figure 6 (a) also illustrates the transmitter (Tx) and receiver (Rx) configuration of the OLT, which is identical to the setup in the ONU. Consequently, the total downstream and upstream capacities are both 100Gb/s and are shared among multiple ONUs using a hybrid TFDM scheme, as shown in Figure 6 (b). Each ONU can achieve a peak data rate of 100Gb/s in both the downstream and upstream, similar to what is achievable in TDM PON. Additionally, the proposed TFDM CPON offers more flexible bandwidth allocation. It enables two-dimensional bandwidth allocation, allowing for the establishment of dedicated channels for end users with, i.e., low-latency or high-capacity requirements.

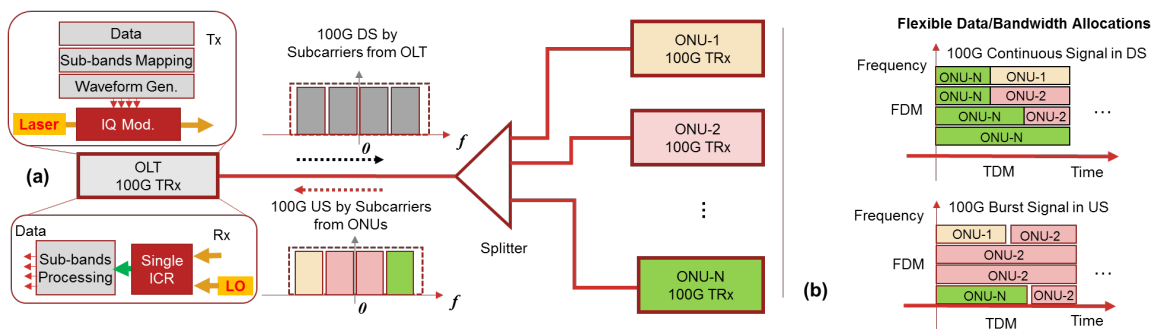


Figure 6 – Principle of TFDM CPON based on digital subcarrier multiplexing scheme: (a) architecture; (b) example of flexible data/bandwidth allocation

Figure 7 (a) and (b) illustrate the digital signal processing (DSP) involved in subcarrier generation on the Tx side and demodulation on the Rx side. In the signal generation process, the data is initially mapped and modulated onto each subcarrier. To reduce the bandwidth on each subcarrier, Nyquist pulse shaping is applied with a 0.1 roll-off factor. Following pre-equalization, the four subcarriers with a baud rate of 6.25 GBd are upconverted to four intermediate frequencies: -15 GHz, -5 GHz, 5 GHz, and 15 GHz. On the receiver side, the inverse processing flow is performed. The subcarriers are first filtered out and separated, and then down converted to baseband. They are processed independently using several key signal recovery functions.

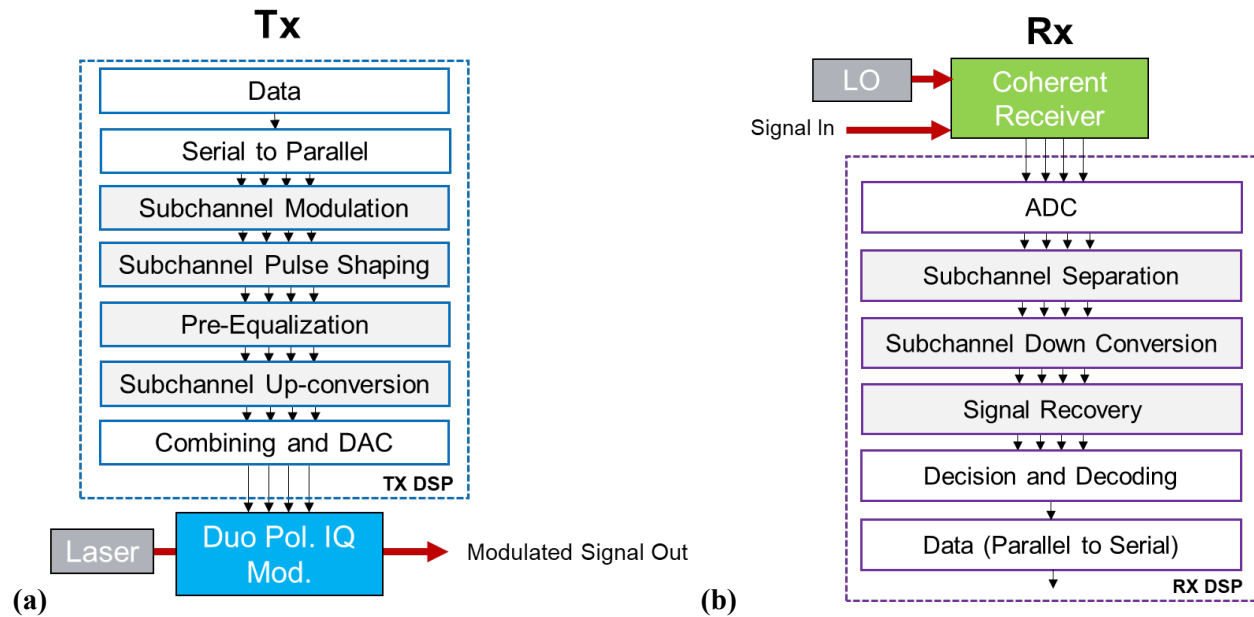


Figure 7 – TFDM DSP flow: (a) Tx subcarrier generation DSP; (b) Rx subcarrier demodulation DSP

The proposed coherent TFDM CPON introduces support for asymmetric ONU/OLT hardware setups and a pay-as-you-go cost model based on bandwidth subscription. Unlike traditional WDM-PON or TWDM-PON, all the ONUs and OLT in the proposed system operate on the same wavelength grid with slight frequency tuning. The coherent detection's inherent wavelength selective feature eliminates the need for optical filtering or wavelength selective components for frequency selection. This coherent TFDM PON system enables more flexible bandwidth sharing utilizing both time and frequency. It is fully compatible with widely deployed TDM PON and can operate on power splitter-based ODNs without requiring additional components. With only one transceiver on the OLT-side and one transceiver on the ONU-side, the system can provide lower overall scheduling latency due to the utilization of frequency division multiplexing.

3. TFDM CPON Key Technology Development

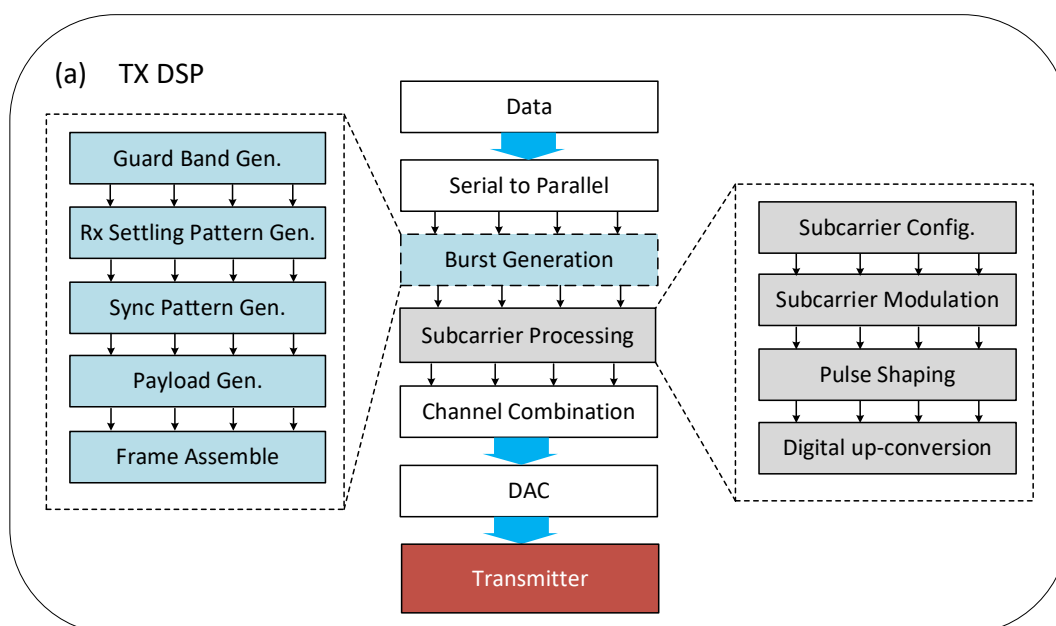
Coherent TFDM technology has undergone significant advancements in past few years, enabling enhanced performance and flexibility in CPONs. In this paper, we highlight three key developments in TFDM technology. Firstly, TFDM Burst Transmitter/Receiver, which is a crucial advancement in TFDM CPONs. This technology enables time domain multiplexing in DSCs, allowing for efficient transmission and reception of burst signals. Secondly, subcarrier frequency window detection and calibration, pre-equalization, and power rebalancing. To maximize the performance of TFDM CPONs, accurate subcarrier frequency window detection and calibration techniques are essential. These methods ensure precise alignment of the frequency windows across the subcarriers, minimizing frequency offset and power imbalance, and improving overall system performance. Lastly, low-cost ONU light sources through remote master tone delivery and optical injection locking. One of the challenges in deploying coherent optics for access networks is the high cost associated with ONU light sources. TFDM technology has introduced a novel solution by leveraging remote master tone delivery and optical injection locking to replace high-cost laser sources and reduce the complexity and cost of coherent ONUs. Through injection locking, the child laser (Fabry-Perot (FP) laser) closely adopts the optical frequency and linewidth characteristics of the parent laser (ECL laser). At the OLT end, seed (or parent/master) laser

sources are generated for both downstream LO and upstream injection carrier seed. Through remote delivery, at the ONU end, only low-cost child lasers are required. Through design, the OIL process can amplify both tones (LO and upstream carrier), eliminating the need for extra optical amplifiers.

These key TFDM technology developments have significantly contributed to the advancement of CPONs. These advancements are expected to drive the adoption of TFDM technology in the emerging era of high-capacity and flexible optical access networks.

3.1. Burst Signal Processing in TFDM Subcarriers

One of the key challenges for TFDM CPON is the realization of upstream coherent burst-mode transmission and detection in DSCs. Figure 8 depicts the DSP processes of coherent TFDM transmitter and receiver that features burst signal processing and burst preamble design. In Figure 8 (a), the TFDM transmitter involves burst frame generation and subcarrier processing, with the former exclusively for upstream transmission. Burst frame generation includes creating patterns for the guard band, receiver settling, synchronization, and payload data. The frames are assigned to DSCs and undergo Nyquist pulse shaping, digital up-conversion, and digital-to-analog signal conversion for transmission. In the TFDM burst receiver as shown in Figure 8 (b), analog signals are down-converted to baseband and subjected to Fast Fourier transform (FFT), digital filtering, and inverse FFT (IFFT). Burst signal detection, primarily for upstream burst reception, starts with power-based frame detection, followed by chromatic dispersion (CD) compensation, clock recovery, and burst frame synchronization. Once the burst signal is received, payload signals are processed using regular coherent receiver DSP methods. The structure of the TFDM signal's burst frame is depicted in Figure 8 (c). A guard time is incorporated between adjacent burst frames. For TFDM signals operating at 6.25 GBd (0.16 ns per symbol), a guard time of 640 symbols (equivalent to 102.4 ns) is allocated. This guard time allows the transmitter (Tx) to be turned on/off as required. When the burst frame initiates, the first portion is dedicated to Rx settling, typically starting with automatic gain control performed by the burst-mode transimpedance amplifier (BM-TIA). Once the BM-TIA reaches a steady-state, the OLT receiver proceeds with burst-mode signal processing for coherent detection of upstream burst signals. The synchronization section encompasses three major components: frame synchronization, state of polarization (SOP) estimation, and frequency-offset estimation (FOE).



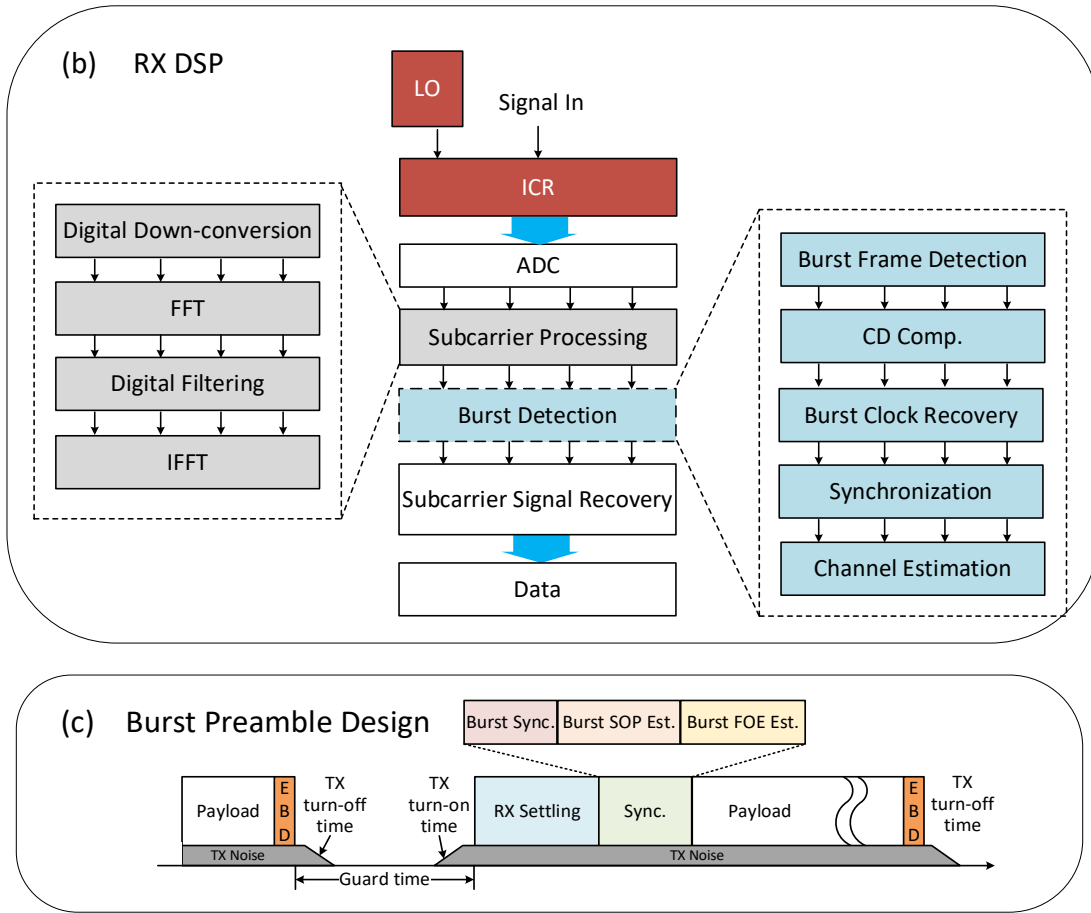


Figure 8 – (a) TFDM burst Tx DSP procedures; (b) TFDM burst Rx DSP procedures; (c) Preamble design in TFDM burst frame

Previous research utilized an auto-correlation based algorithm for TDM burst synchronization, demonstrating good performance [16]. In this study, a double-correlation based algorithm is employed for TFDM burst signal synchronization. This approach aims to achieve more stable and robust burst detection, especially when dealing with significant carrier frequency offset (CFO) and CD resulting from fiber transmission [17]. The synchronization peak $L(\mu)$ using the double-correlation method can be mathematically expressed as Equation (1):

$$L(\mu) = \sum_{i=1}^{L-1} \left\{ \sum_{k=i}^{L-1} |r_{\mu+k}^* s_k r_{\mu+k-i} s_{k-i}^*| - \sum_{k=\mu+i}^{\mu+L-1} |r_k| |r_{k-i}| \right\} \quad (1)$$

In this equation, $\{s_k\}$ represents a fixed frame synchronization pattern with a length of L symbols, and $\{r_k\}$ denotes the received signal [17]. However, when the sync frame length L is large, the computational complexity becomes impractical for real-world applications due to the high number of iterations required by $L-1$. To address this, the $L-1$ term is replaced with a factor M , representing the number of iterations in the double-correlation algorithm, where $1 \leq M < L-1$. This modification allows for a more feasible calculation as demonstrated in Equation (2):

$$L(\mu) = \sum_{i=1}^M \left\{ \sum_{k=i}^M |r_{\mu+k}^* s_k r_{\mu+k-i} s_{k-i}^*| - \sum_{k=\mu+i}^{\mu+M} |r_k| |r_{k-i}| \right\} \quad (2)$$

In Equation (2), the M-factor represents the number of iterations in the double-correlation synchronization algorithm. Increasing the M value enhances the performance of the algorithm, but it also leads to a substantial increase in computational complexity. To strike a balance between synchronization robustness and computational complexity, we have selected M=4 for the subsequent experiments.

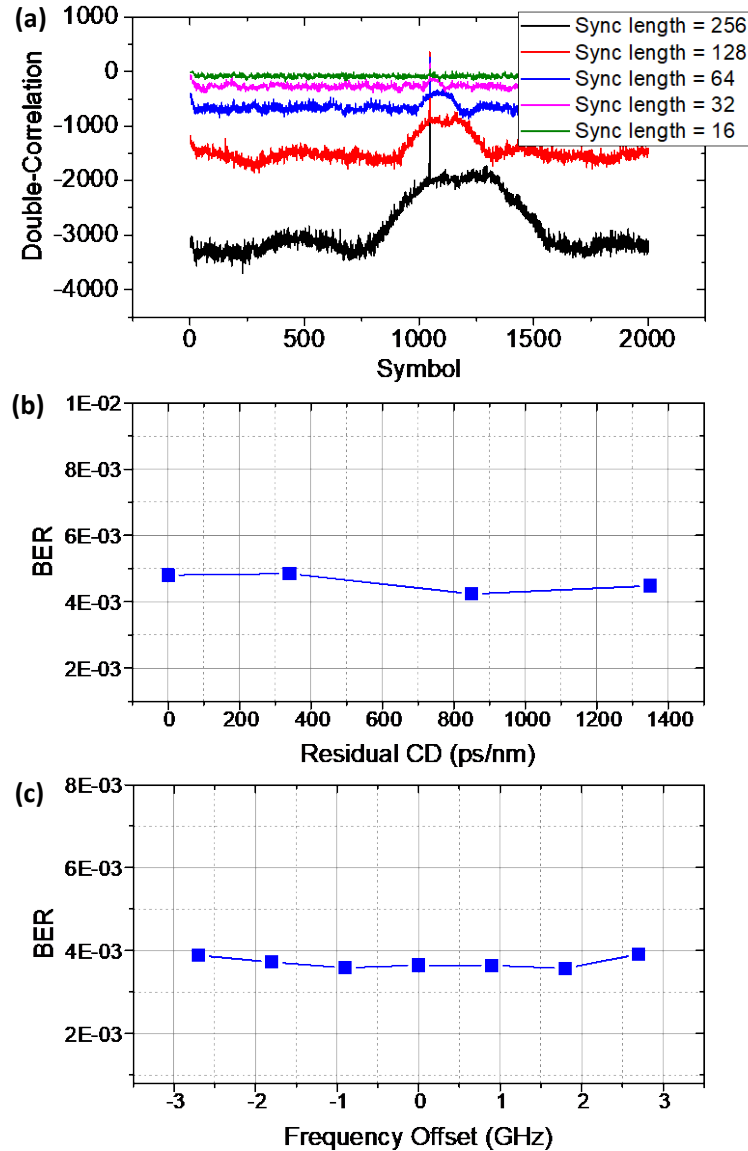


Figure 9 – TFDM burst optimization and performance evaluation: (a) Double-Correlation pattern in TFDM burst operation under different synchronization symbol length; (b) TDM burst BER performance under residual CD; (c) TDM burst BER performance under CFO

To examine the effect of the burst preamble design on the performance of the TFDM system, we conducted experiments using various lengths of preambles. For the Rx settling section, we utilized Rx settling length in number of symbols of 1024, 512, and 256, which correspond to time durations of 163.84 ns, 81.92 ns, and 40.96 ns, respectively (assuming a symbol rate of 6.25 GBd, where 1 symbol equals 0.16 ns). To achieve reliable synchronization, we tested sync length of 256, 128, 64, 32, and 16 symbols, corresponding to time durations of 40.96 ns, 20.48 ns, 10.24 ns, 5.12 ns, and 2.56 ns, respectively. In

Figure 9 (a), a collection of double-correlation patterns illustrates the TFDM burst operation at different synchronization lengths: 256, 128, 64, 32, and 16 symbols. It is worth noting that the length of the Rx settling does not significantly impact the synchronization results. Consequently, the results presented in Figure 9 (a) employ an Rx settling length of 512. Based on the observations in Figure 9 (a), for a reliable and consistent synchronization of the TFDM coherent burst, the synchronization length in symbols should be greater than 32, corresponding to a duration of 5.12 ns. We also evaluated the performance of the proposed synchronization algorithm for the TFDM burst receiver in the presence of transmission impairments, such as CD or CFO. Figure 9 (b) illustrates the system bit error rate (BER) under different residual CD values caused by varying fiber transmission distances. The results indicate that the double-correlation synchronization algorithm ensures stable operation even with uncompensated CD, as no significant impact on performance was observed. Figure 9 (c) presents the BER results at different CFO values. Similar to the CD test results, the presence of CFO does not affect synchronization or system BER performance. It is important to note that the TFDM burst receiver incorporates channel recognition and frequency-window calibration processes that will be discussed in the following section. These processes enable accurate calibration of TFDM subcarrier frequency windows and enhance the receiver's tolerance to carrier frequency detuning.

3.2. Subcarrier Recognition, Pre-equalization, and Power Rebalancing

In TFDM, laser drifting leads to subcarriers not being at their desired locations, especially in the ONU upstream direction in the case of different ONUs have independent laser sources. Drifting and collisions between adjacent subcarriers can result in crosstalk and must be avoided to prevent system outages. On the other hand, At the OLT receiver's end, power imbalances between DSCs coming from different end nodes result in additional penalties. To overcome the challenges posed by power imbalances between subcarriers in a system, as well as random frequency drifting caused by laser diodes in different ONUs, a novel TFDM burst transceiver algorithm has been proposed and experimentally demonstrated. This transceiver incorporates several key features, including subcarrier pre-equalization, power rebalancing, and frequency window detection and calibration. Figure 10 illustrates the processes involved in the proposed CPON TFDM receiver and transmitter, which consist of three main functions: 1) channel recognition and frequency window calibration (CR-FC), 2) channel pre-equalization (Pre-EQ), and 3) channel power rebalancing (PR).

Figure 10 (a) provides a detailed description of the CPON TFDM burst receiver in the OLT. In the receiver, CR-FC occurs between the analog-digital conversion (ADC) and subcarrier down conversion stages. The CR-FC process begins by extracting a set of 4096 points from the received data stream, which are then transformed into the frequency domain using Fast Fourier transform (FFT). The next step involves smoothing the channel distribution in the frequency domain and generating a binary spectrum map. In this binary map, 0s represent signal components below a preset threshold, while 1s represent signal components above the threshold. The binary spectrum map, along with a set of predefined rules, helps eliminate noise peaks, optical carrier residue, and harmonics in the frequency domain. The channel boundaries are determined by identifying abrupt changes on the binary map. By locating rising and falling edges on each frequency channel, the carrier frequencies are calculated, and the frequency windows are calibrated accordingly.

With CR-FC completed, the optical power in each subcarrier is estimated by integrating the square of the absolute signal values within each calibrated frequency window. This power estimation is then transmitted downstream and utilized for subcarrier power rebalancing in subsequent processes. The next steps in the receiver include digital down conversion, baseband filtering, burst detection by locating and synchronizing the burst signals in each subcarrier, and coherent DSP for upstream signal recovery. Within the subcarrier DSP, the channel response is extracted during the execution of the constant modulus

algorithm (CMA). The OLT sends control signal feedback to the ONU, which includes the estimated power information obtained from the CR-FC step and the channel response acquired from CMA. Figure 10 (b) illustrates the DSP process in the ONU transmitter, where the control signal feedback received from the OLT is utilized for performing Pre-EQ and PR during subcarrier data processing. Using the channel response information provided by the control signal, Pre-EQ is implemented by applying a reverse channel response to the signals. This step adjusts the signal amplitudes in the ONU transmitter based on the received channel response. Subsequently, the ONU transmitter utilizes the estimated power information obtained from the CR-FC step to further adjust the signal amplitudes. This adjustment ensures a completely rebalanced optical power distribution among the subcarriers.

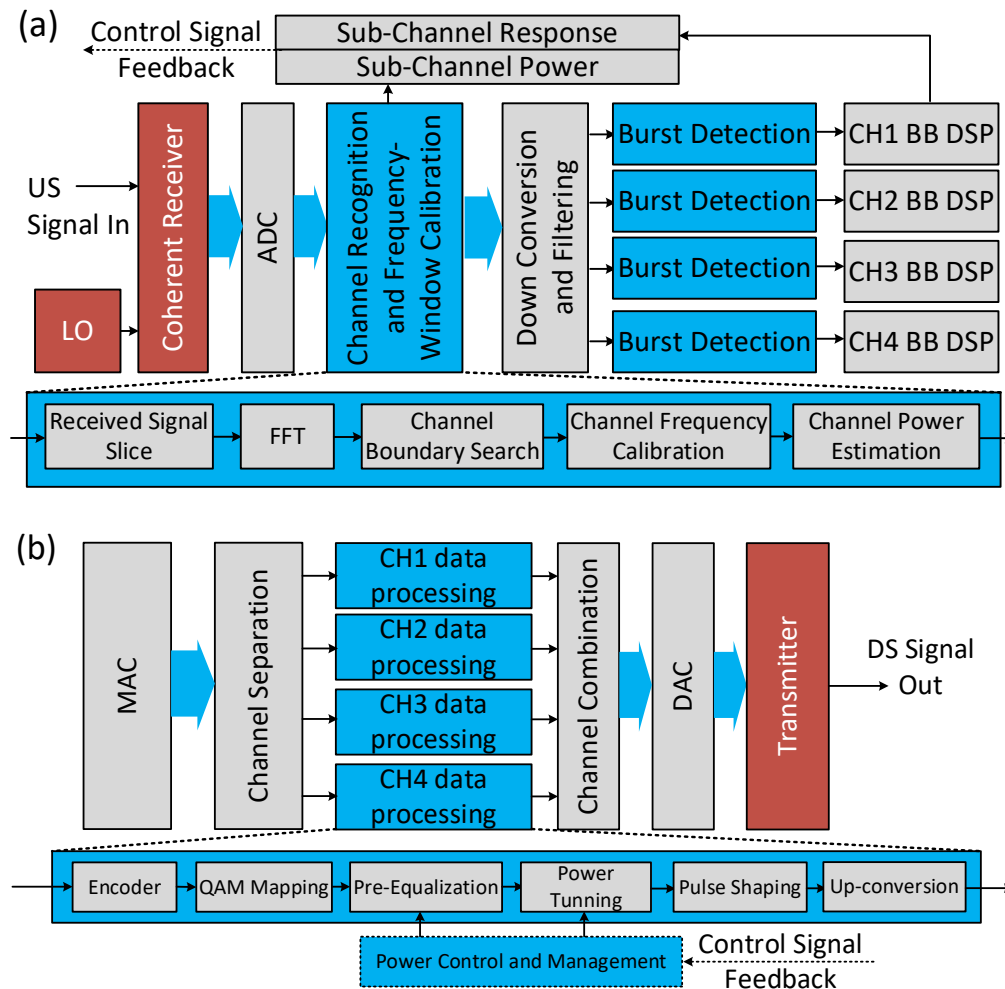


Figure 10 – Proposed DSP procedures featuring subcarrier recognition, pre-equalization, and power rebalancing in: (a) TFDM coherent burst receiver; (b) TFDM coherent transmitter

Figure 11 displays the electrical spectra of TFDM signals and illustrates the process of subcarrier recognition, pre-equalization, and power rebalancing. In the unprocessed TFDM signal depicted in Figure 11 (i), the spectrum and power distribution in the frequency domain are uneven. The first step of the process involves performing CR-FC to identify the boundaries of the subcarriers, as shown in Figure 11 (ii). Following CR-FC, subcarrier pre-equalization (Pre-EQ) is carried out by applying the reverse response of the subcarrier information obtained from the CMA step. This Pre-EQ step results in a

flattened signal within each subcarrier, as illustrated in Figure 11(iii). Once the subcarrier boundaries are identified and accurate power control is achieved through Pre-EQ, the final step is to rebalance the power in each subcarrier by adjusting the transmitter signal amplitude at the ONUs. As a result of this power rebalancing, a fully rebalanced TFDM signal spectrum is obtained, as depicted in Figure 11 (iv).

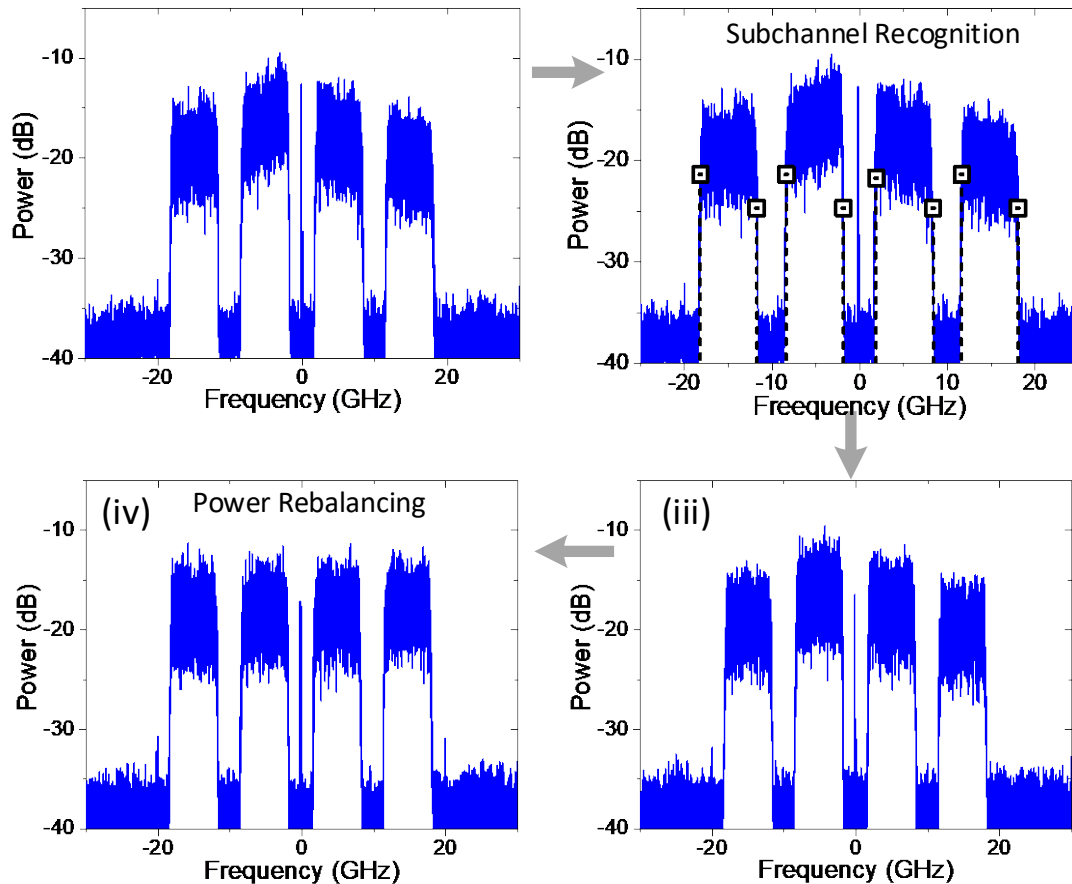


Figure 11 – Process of CR-FC, Pre-EQ, and PR of TFDM signal

Figure 12 demonstrates the performance of the proposed CR-FC algorithm. In Figure 12 (a), we intentionally shifted the center frequency of one subcarrier (CH3) by 2.2 GHz from its original frequency. With the implementation of CR-FC, the boundaries of CH3, as well as other channels, were successfully identified. Figure 12 (b) presents BER performance of upstream transmission plotted against CH3 frequency detuning, ranging from -2.4 to +2.4 GHz. To assess the performance of CR-FC, we compare three methods for CFO estimation and correction: 1. Conventional fourth-power carrier estimation (FPCE) at baseband (BB) DSP after down conversion; 2. Frequency-pilot-tone-based CFO estimation, where pilot tones are inserted at -20, -10, 10, and 20 GHz, followed by FPCE in the BB DSP; and 3. The proposed CR-FC followed by FPCE in the BB DSP. Based on the BER performance depicted in Figure 12 (b), using only FPCE exhibits the lowest CFO tolerance, primarily due to the reduction in frequency detection range caused by the fourth-power operation. Pilot-tone + FPCE improves CFO estimation and correction performance. However, when encountering a large CFO, the pilot tones end up overlapping with adjacent sub-channels, limiting the CFO tolerance. In contrast, the proposed CR-FC + FPCE demonstrates significantly improved CFO tolerance and outperforms the other two methods. The CR-FC algorithm, showcased in Figure 12, provides subcarrier detection and frequency window calibration

across a wide frequency range. It plays a crucial role in facilitating dynamic burst detection and enhances the TFDM system's ability to tolerate CFO variations.

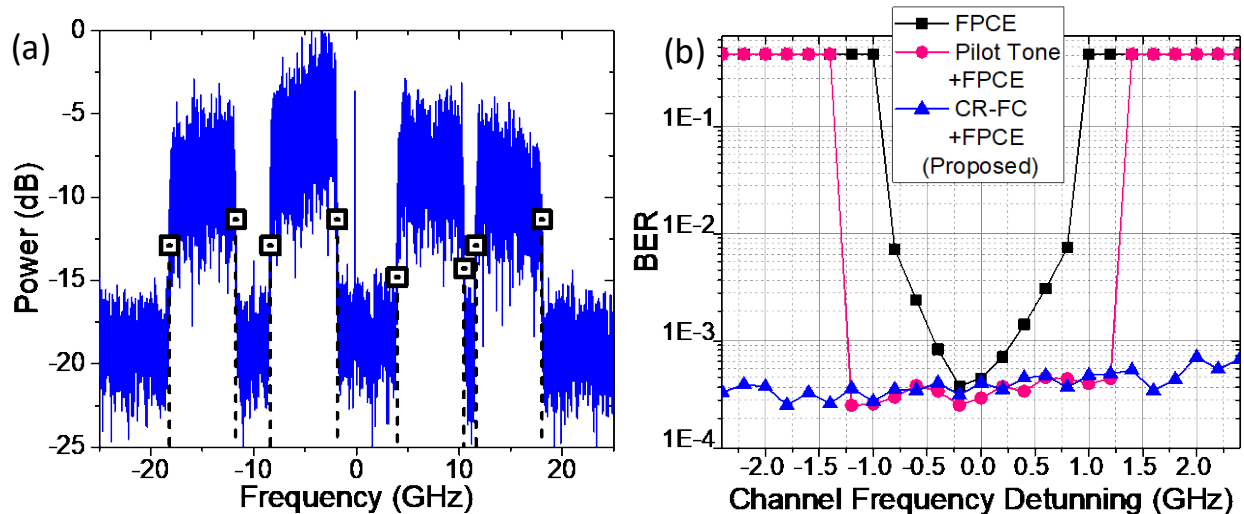


Figure 12 – CR-FC algorithm performance: (a) channel boundary detection with large CFO; (b) BER versus frequency detuning using different methods

Figure 13 illustrates the test results of BER performance versus received optical power (ROP) for a TFDM CPON optical link utilizing 80 km of single-mode fiber (SMF). Figure 13 (a) displays the BER versus ROP curves for all four subcarriers transmitted from two ONUs, both with and without the implementation of Pre-EQ and PR algorithms. Without Pre-EQ and PR, a noticeable difference in power budget of up to 4 dB can be observed among the subcarriers. However, with the application of Pre-EQ and PR, the power budget difference between the subcarriers is minimized, resulting in an overall improvement in system performance. Figure 13 (b) showcases the BER versus ROP performance for the system with Pre-EQ and PR in two scenarios: back-to-back (B2B) transmission and 80 km fiber transmission. In both cases, for all ONUs and subcarriers, the transmission over the 80 km fiber link does not introduce any significant penalty in terms of BER performance. The plot also includes reference points such as the staircase hard-decision (HD) forward error correction (FEC) threshold ($BER = 4.5E-3$) [18] and the concatenated soft-decision (SD) FEC threshold ($BER = 1E-2$) [19] for comparison. Overall, the results depicted in Figure 13 highlight the positive impact of Pre-EQ and PR algorithms on minimizing power budget differences between subcarriers and improving the BER performance of the TFDM CPON optical link, even over long-distance fiber transmissions.

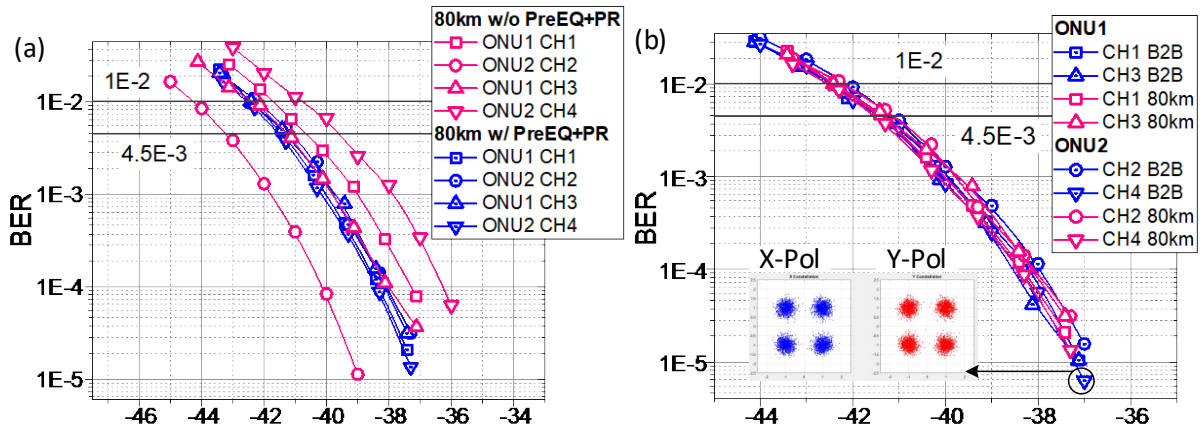
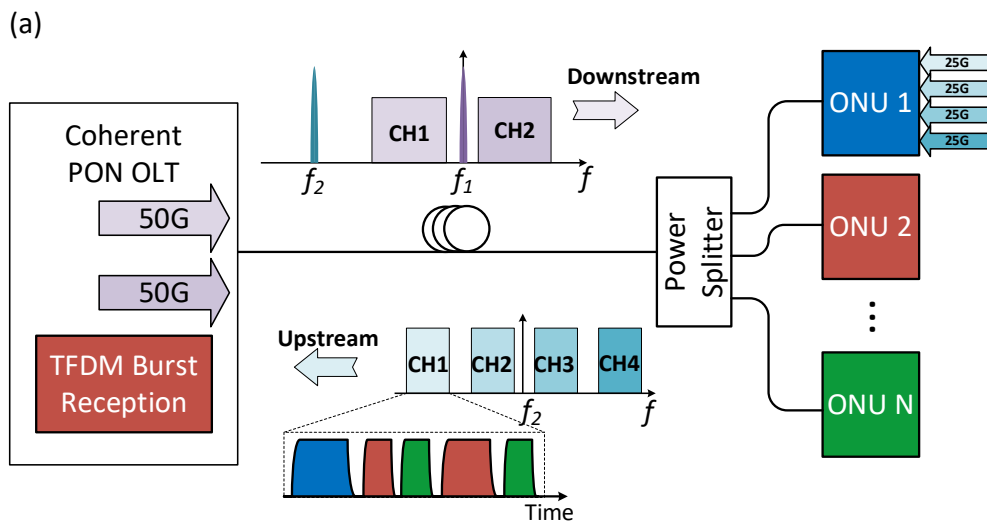


Figure 13 – (a) BER performance with and without Pre-EQ + PR; (b) BER performance

3.3. ONU Cost Reduction Through Remote Optical Carrier Delivery

Despite efforts to simplify coherent optics for short-haul applications, the high cost of current products remains the primary barrier to widespread adoption in access networks. One major cost contributor is the use of high-quality optical sources, such as external cavity lasers (ECLs) which are essential components of coherent modules. However, optical injection locking (OIL), a technique that locks a laser to an external optical tone through injection of external light, presents an opportunity for low-cost coherent optics in PON applications, especially for customer premise devices. Leverage OIL and TFDM subcarriers, we propose and experimentally demonstrate a new TFDM CPON architecture that involves delivering two optical tones to the ONUs from a remote location. By amplifying these optical tones using OIL, we can provide the ONU with an optical carrier and a local oscillator (LO), effectively replacing expensive lasers like ECLs with affordable Fabry-Perot laser diodes (FP-LDs). Experimental investigation shows that the proposed architecture performs comparably to a regular ECL-based system, without any significant degradation in performance. Furthermore, this architecture offers the advantage of frequency synchronization between the ONU light sources and the OLT lasers, which helps mitigate random frequency drifts caused by independently operated lasers in ONUs.



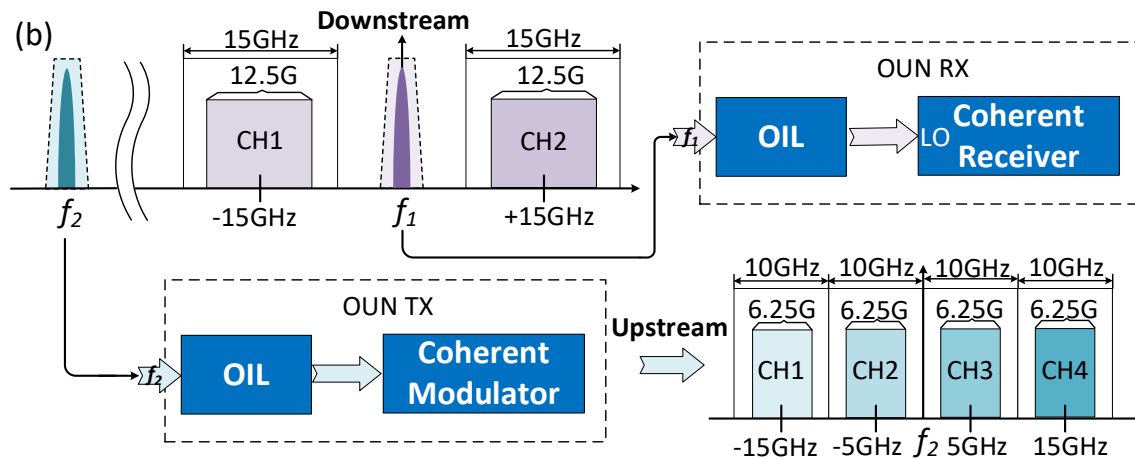


Figure 14 – (a) TFDM CPON scheme with remote optical tone delivery; (b) subchannel design for DS and US transmission

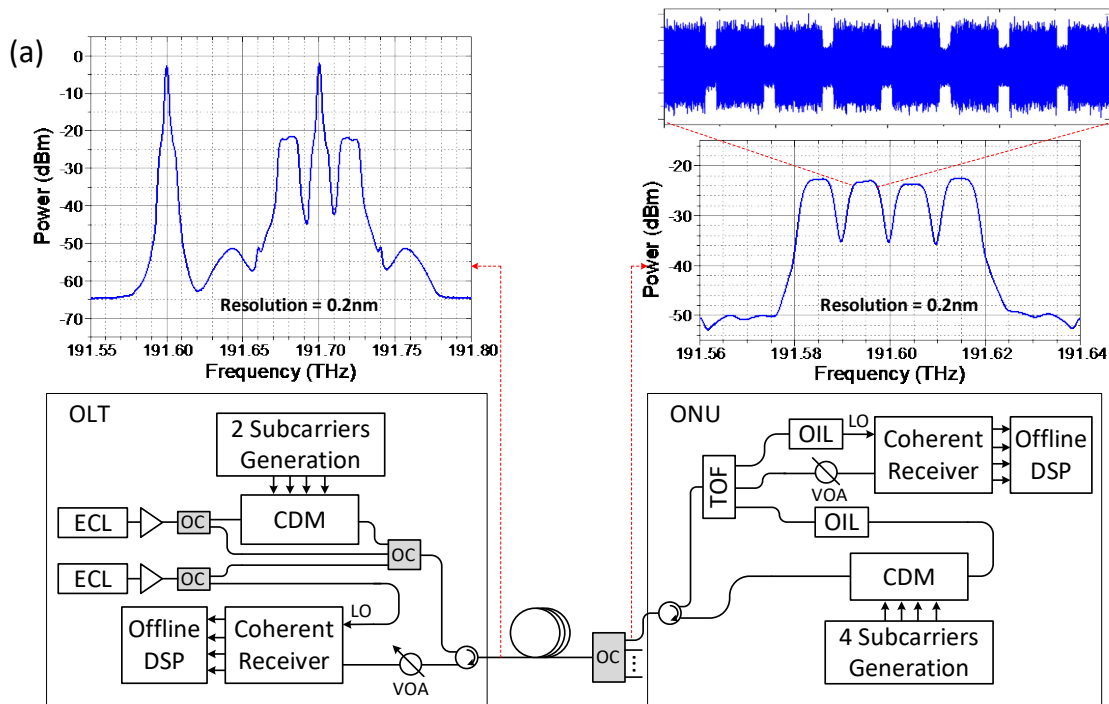
Figure 14 (a) illustrates the basic concept of the proposed TFDM CPON architecture with remote optical tone delivery. By utilizing the flexible bandwidth allocation capability of TFDM CPON, various subcarrier configurations can be employed to accommodate different capacities and link budgets. In the downstream direction, two TFDM subcarriers are generated on a single wavelength in the OLT. Two unmodulated optical tones centered at frequencies f_1 and f_2 for remote delivery are combined with the TFDM subcarriers for downstream transmission. One of the optical tones at frequency f_1 , which matches the optical carrier frequency of the downstream TFDM signal, is used to generate the LO for downstream signal detection at the ONU through OIL. The other optical tone at frequency f_2 is employed to generate an optical carrier through OIL at the ONU for upstream signal transmission. Importantly, both tones are amplified during the OIL process, eliminating the need for an additional optical amplifier. In the upstream direction, four TFDM subcarriers are generated at the ONU, utilizing a carrier frequency of f_2 . Figure 14 (b) depicts the arrangement of the TFDM subcarriers. The two subcarriers designated for downstream transmission occupy two 15 GHz frequency windows centered at -15 and +15 GHz with respect to f_1 . Each downstream subcarrier is modulated with a 50 Gb/s dual-polarization (DP) quadrature phase shift keying (QPSK) signal at a baud rate of 12.5 GBd, resulting in an aggregate downstream data rate of 100 Gb/s. In the upstream direction, the four subcarriers are each distributed within a 10 GHz frequency window, with center frequencies at -15, -5, +5, and +15 GHz relative to f_2 . Each upstream subcarrier is modulated with a 25 Gb/s DP-QPSK signal at a baud rate of 6.25 GBd, yielding an aggregated upstream data rate of 100 Gb/s. The frequency spacing between f_1 and f_2 is set to 100 GHz to align with the ITU DWDM (dense wavelength division multiplexing) frequency grid.

Figure 15 (a) shows the experimental configuration of the proposed TFDM CPON. Two ECLs serve as the light sources at the OLT. One ECL generates downstream TFDM signals using a coherent driver modulator (CDM), while the other ECL provides the LO for upstream signal detection at the OLT receiver. The ECL outputs also serve as optical master tones for injection locking at the ONUs. To establish the experimental setup, a 50 km fiber link and a 1x32 passive optical splitter are employed for the optical distribution network (ODN). At the ONU side, a multiport tunable optical filter (TOF) is utilized to separate the downstream TFDM signals and the two optical tones. The downstream TFDM signals are detected by a coherent homodyne receiver using the LO generated through OIL. The upstream TFDM signals, on the other hand, are transmitted using another OIL setup coupled to a CDM. Both the downstream and upstream signals undergo offline DSP using appropriate codes. The optical spectra of the downstream (broadcast) and upstream (burst) TFDM signals are depicted in the insets of Figure 15 (a). Although the experiment employs off-the-shelf discrete components for demonstration purposes, it is

worth noting that advanced photonic integration platforms have the potential to combine these components, leading to the development of low-cost commercial products.

To demonstrate the effectiveness of using an OIL laser as the ONU LO for downstream signal detection, the BER performance was measured against ROP per channel for downstream TFDM subcarriers. The experiments were conducted over a 50 km fiber transmission with a 32-way optical splitter, and the results of one subcarrier (CH1) are shown in Figure 15 (b). Note that the performance of the other TFDM subcarrier (CH2) is almost identical and is therefore not shown here for simplicity. Additionally, back-to-back (B2B) BER versus ROP measurement was carried out using the OIL LO. The performance of the system using a regular ECL as the LO was also included in the charts, along with reference thresholds for staircase HD FEC (BER = 4.5E-3) and concatenated SD FEC (BER = 1.2E-2). The goal was to compare the performance of the proposed architecture with remotely delivered optical tone and OIL for ONU LO against the performance of a system using a regular ECL LO. The experimental results demonstrated the functionality of the proposed architecture in downstream transmission. It was observed that there was no significant degradation in performance when using the remotely delivered optical tone in conjunction with OIL for ONU LO, as compared to using a regular ECL LO.

Figure 15 (c) presents the results of BER versus ROP per channel for upstream burst TFDM signals (CH1, other subcarriers perform nearly identical and will not be shown here) using an OIL-based ONU transmitter enabled by the remotely delivered optical tone. The results include both fiber transmission (50 km/32 split) and B2B scenarios. Additionally, the BER performance of the subcarrier using a regular ECL as the transmitter laser is included for comparison. Similar to the downstream broadcasting results discussed earlier, the upstream burst transmission employing the proposed OIL-based transmitter demonstrates minimal performance degradation. Overall, the experimental findings indicate that the proposed OIL-based transmitter/LO, utilizing the remotely delivered optical tone, achieves comparable performance to a traditional ECL-based transmitter/LO in terms of BER, both at the HD-FEC threshold and the SD-FEC threshold.



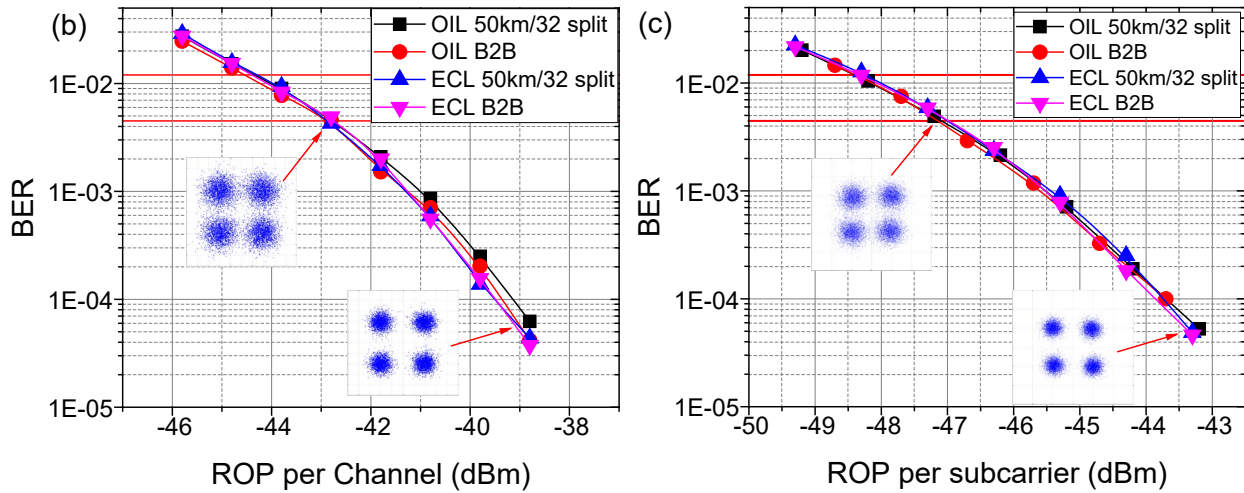


Figure 15 – (a) Experimental setup with optical spectrums of TFDM DS and US channels; (b) BER versus ROP in downstream; (c) BER versus ROP in upstream

The proposed OIL-based system offers an additional advantage by achieving frequency locking between the ONU transmitter/LO and the OLT light sources. This leads to minimal optical frequency offset between them. In contrast, a regular ECL-based system exhibits a much larger carrier frequency offset (CFO) of approximately 0.34 GHz, as depicted in Figure 16 (a). This substantial CFO makes signal recovery impossible without CFO compensation. On the other hand, the proposed OIL-based system demonstrates a residual CFO of only 0.12 MHz, enabling simplification of the coherent receiver DSP by eliminating the need for CFO compensation. This simplification is achieved without significant performance degradation. Figure 16 (b) illustrates the BER performance of the OIL-based system without CFO compensation for both downstream and upstream burst transmissions. In comparison to the ECL-based system with CFO compensation, the OIL-based system exhibits similar performance levels. However, it offers the significant advantages of simplified receiver DSP complexity and cost savings in ONU hardware.

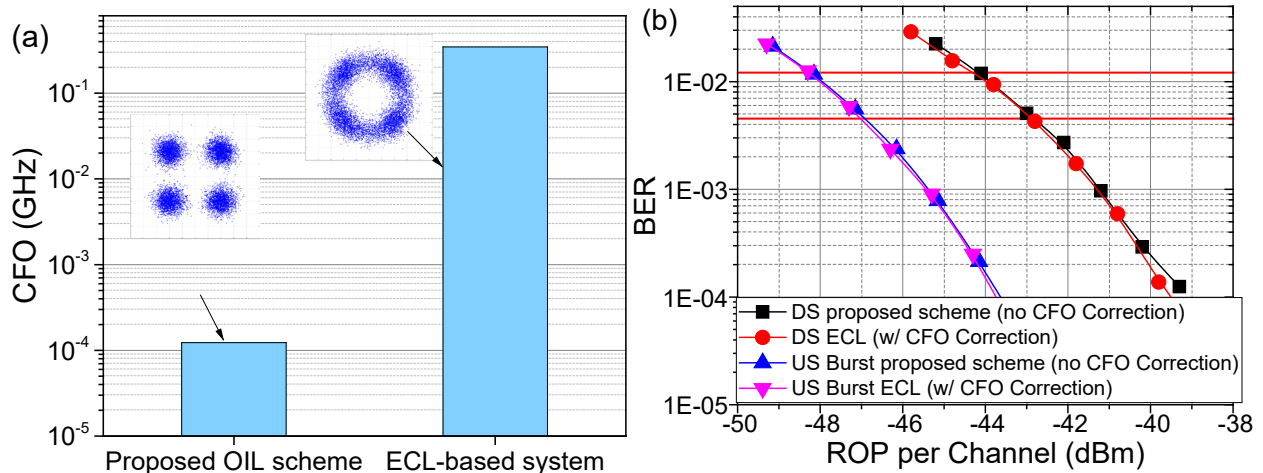


Figure 16 – (a) Residual CFO for proposed OIL scheme vs. regular ECL-based system; (b) BER vs. ROP per channel for proposed OIL scheme without CFO correction compared with regular ECL-based system with CFO correction

4. Advantages, Challenges, and Discussions

DSC based TFDM is a promising advancement in optical transmission technology and architecture that leverages subcarrier implementation in digital domain to enhance data transmission flexibility and efficiency. In this part, the benefits of subcarrier implementation in TFDM are summarized, including efficient bandwidth granularity and utilization, flexible link budget designs, low-latency dedicated bandwidth services, reduced power consumption, and scalable architecture. However, the implementation of TFDM also introduces challenges such as subcarrier frequency and gain control, impairment calibration to mitigate frequency mirroring, increased complexity of DSP and scheduling control, and transmitter power reduction due to modulation clipping, as shown in Figure 17. Balancing these benefits and challenges is crucial for the industry to harness the long-term potential of TFDM while addressing current market demands and infrastructure readiness.

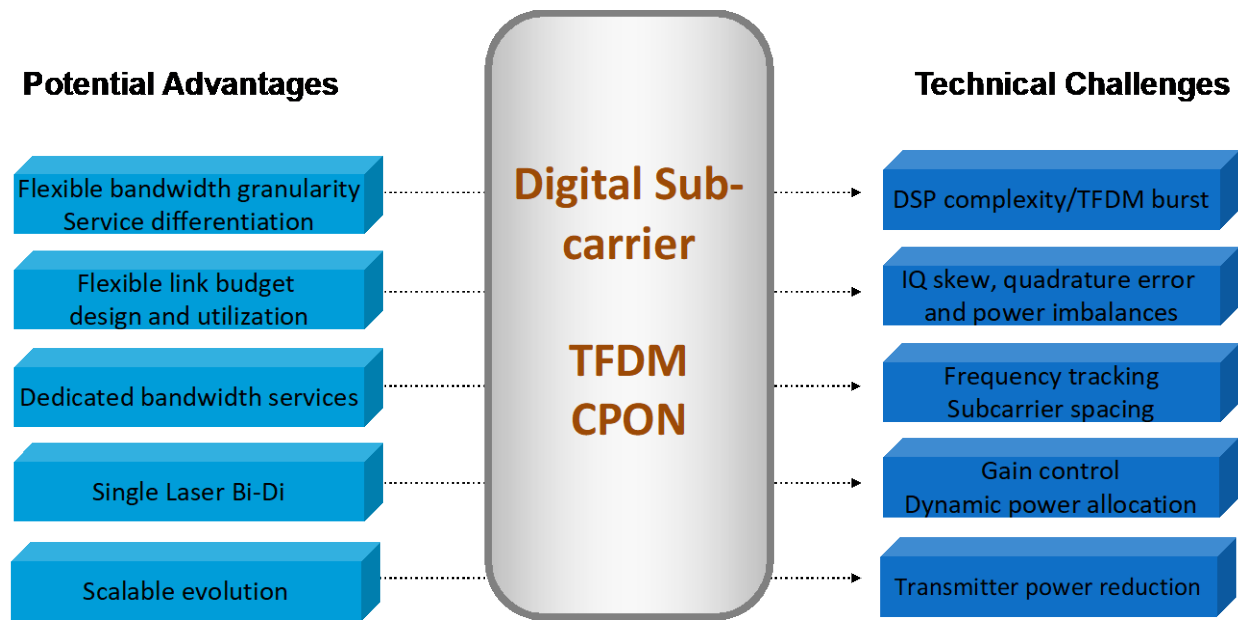


Figure 17 – Technical summary of DSC based TFDM CPON

DSC implementation can enhance bandwidth utilization compared to traditional single-carrier options. The finer granularity of subcarriers, leads to finer data capacity quantization, thereby reducing data wastage and allowing for increased data throughput within a given bandwidth allocation. Subcarrier implementation opens the door to flexible link budget in the PON designs, fostering improved network performance. The allocation of subcarriers can be optimized to achieve specific outcomes. For example, by allocating 50% of the subcarriers to carry 50% of the overall aggregated capacity, a 3dB additional link budget can be achieved by transmitting the similar amount of optical power as 100% subcarriers. Additionally, the emphasis of subcarrier power in the downlink can be effectively managed to balance power allocation across the network.

A subcarrier model provides a way to achieve low latency and/or high security dedicated bandwidth services through segmentation in subcarriers and their configuration for specific service needs while utilizing the same optical PON infrastructure. This model can be reconfigured on a per ODN basis, enabling tailored services to meet varying demands. DSC implementation also contributes to reduced power consumption, particularly during periods of lower peak bandwidth demands. The design of a DSP that scales power utilization based on active DSC usage enhances energy efficiency. The incorporation of

DSCs establishes a scalable architecture that allows for independent expansion of OLT and ONU bandwidth options through increasing the supported number of subcarriers.

The flexibility and efficiency of this TFDM approach come with technical implementation challenges. Despite the substantial advantages subcarriers provide, certain hurdles emerge, particularly in the domain of subcarrier frequency control. The possibility of collisions between neighboring subcarriers introduces the risk of crosstalk, which could potentially lead to disruptions in the system's operation. To mitigate such issues, the allocation of adequate guard bands and meticulous management of laser jitter become essential prerequisites. Ensuring uniform signal strength across DSCs is also essential for optimal system performance. A per subcarrier gain control mechanism on both the transmitter and receiver sides is necessary to equalize the power of received DSC channels before subsequent DSP processing [20].

Additional impairments stemming from manufacturing and initialization processes, such as frequency mirror image due to IQ skew, quadrature error, and IQ power imbalances, need to be accurately calibrated out to maintain signal integrity and quality. Further, modulation clipping, resulting from the enhanced peak-to-average power ratio (PAPR) in the multiple subcarrier scheme, can lead to a reduced fiber link budget due to the reduction in the transmitter output power. Careful system-level consideration and optimization are necessary to mitigate this impact. It is also noted that the introduction of subcarriers introduces complexity to DSP and scheduling control systems. The need for 2-dimensional resource scheduling to manage diverse subcarriers adds intricacy to system design and management.

DSC TFDM has the potential to transform the landscape of coherent optical technology application in the access networks. The benefits of subcarrier implementation, including enhanced bandwidth utilization, flexible link budget designs, and low-latency services, are compelling. However, the challenges related to subcarrier frequency and gain control and others must be addressed. Achieving equilibrium between the enduring merits of TFDM and the pragmatic factors of market demand, infrastructure preparedness, and economic viability is pivotal to shaping the future of coherent optical transmission systems and networks.

5. Conclusions

In this paper we present the TFDM technology in the context of CPONs. The CableLabs CPON project, initiated in May 2021, aims to future-proof cable's access architecture by developing specifications for 100G PONs and multi-vendor interoperable devices. Currently two data multiplexing methods are being considered for emerging CPONs: TDM and DSC-based FDM combined with TDM. While the traditional TDM approach has been widely deployed in existing PONs, it faces challenges in future CPONs due to potentially high scheduling latency and limited flexibility. In contrast, the TFDM solution, which combines the benefits of TDM and FDM by utilizing subcarriers in the frequency domain, enables the allocation of different frequency bands to network services or ONU groups with varying latency and capacity requirements while maintaining the simplicity of traditional grant request and bandwidth allocations techniques. This approach eliminates the need of contention resolution, significantly improves scheduling latency and traffic blocking rates, and facilitates the coexistence of mobile and video streaming services on a converged CPON platform with enhanced flexibility. The advantages associated with incorporating TFDM subcarriers, such as improved bandwidth utilization, adaptable link budget configurations, low power consumption, and dedicated channel for low-latency services, are compelling. Nevertheless, the hurdles linked to managing subcarrier frequencies and gains, among other technical challenges, necessitate resolution. Attaining a balance between the strengths of TFDM and the practical considerations of market requirements, infrastructure readiness, and economic feasibility stands as a critical factor in shaping the development of coherent optical transmission systems and networks in the future.

This paper reviews the technology concept of TFDM CPONs, which support asymmetric ONU/OLT hardware configurations and pay-as-you-go ONU cost based on bandwidth subscription. Unlike traditional WDM-PON or TWDM-PON, the coherent TFDM-PON system operates at the same wavelength grid with slight frequency tuning, ensuring compatibility with widely deployed TDM-PONs and power splitter-based ODNs. Additionally, key technology developments in TFDM CPONs are discussed: Firstly, a burst transmitter/receiver for TFDM CPON enables the time domain multiplexing and processing inside DSCs. Secondly, frequency window detection and calibration schemes, along with pre-equalization and phase recovery, enhance the tolerance to carrier frequency detuning and effectively minimize the power budget differences between subcarriers. Lastly, a novel TFDM CPON architecture addresses a major challenge in deploying coherent optics for access networks by providing low-cost ONU light sources through remote master tone delivery and optical injection locking. The major advantage is to have the opportunity of an asymmetric design where complexity, performance and capabilities are moved to the OLT while the ONU complexity is kept low.

The advancements achieved in TFDM technology establish it as a strong contender for forthcoming next-generation CPONs, offering capacities of 100G and beyond. This promises adaptable bandwidth distribution across temporal and spectral dimensions over a single coherent transceiver. Furthermore, this study delves into the advantages, challenges, and potential remedies linked to DSC integration within TFDM systems. By tackling these challenges in conjunction with sound business strategies, it becomes very promising that TFDM-based CPONs possess the capability to fortify optical access architecture for the future.

6. Acknowledgements

Special acknowledgments for fruitful discussions and assistance with all Aspects of this study: Dr. Curtis Knittle, Chris Stengrim, Matt Schmitt, Karthik Sundaresan, Steve Goeringer as well as the dedicated members of the Working Group (WG) and Operator Advisory Group (OAG) from CableLabs CPON Project.

Abbreviations

ADC	analog-to-digital converter
B2B	back-to-back
BER	bit error rate
CD	chromatic dispersion
CDM	coherent driver modulator
CFO	carrier frequency offset
CMA	constant modulus algorithm
CPON	coherent passive optical network
CPR	carrier phase recovery
CR-FC	channel recognition and frequency window calibration
DAC	digital-to-analog converter
DSC	digital subcarrier
DSP	digital signal processing
DWDM	dense wavelength division multiplexing
ECL	external cavity laser
FEC	forward error correction
FFT	Fast Fourier transform
FOE	frequency-offset estimation
FP-LD	Fabry-Perot laser diode
FTTH	fiber to the home
Gb/s	gigabits per second
IM-DD	intensity modulation and direct detection
ODN	optical distribution network
OIL	optical injection locking
OLT	optical line terminal
ONU	optical network unit
P2MP	point-to-multipoint
PAPR	peak-to-average power ratio
PMD	polarization-mode dispersion
PON	passive optical network
PR	power rebalancing
Pre-EQ	pre-equalization
QAM	quadrature amplitude modulation
QPSK	quadrature phase shift keying
ROP	received optical power
Rx	receiver
SOP	state of polarization
TDM	time-division multiplexing
TFDM	time-and-frequency-division multiplexing
TWDM	time-and-wavelength-division multiplexing
Tx	transmitter
TOF	tunable optical filter
WDM	wavelength-division multiplexing

Bibliography & References

- [1] Z. Jia and L. A. Campos, "Coherent Optics for Access Networks," Routledge & CRC Press, Nov. 01, 2019.
- [2] Z. Jia and L. A. Campos, "Coherent Optics Ready for Prime Time in Short-Haul Networks," IEEE Network, vol. 35, no. 2, pp. 8–14, 2021.
- [3] J. Zhang and Z. Jia, "Coherent Passive Optical Networks for 100G/λ-and-Beyond Fiber Access: Recent Progress and Outlook," in IEEE Network, vol. 36, no. 2, pp. 116-123, March/April 2022.
- [4] N. Suzuki, H. Miura, K. Matsuda, R. Matsumoto and K. Motoshima, "100 Gb/s to 1 Tb/s Based Coherent Passive Optical Network Technology," in Journal of Lightwave Technology, vol. 36, no. 8, pp. 1485-1491, 15 April 15, 2018.
- [5] IEEE 802.3ca, Physical Layer Specifications and Management Parameters for 25 Gb/s and 50 Gb/s Passive Optical Networks, 2020.
- [6] ITU-T G.9804.2, Higher Speed Passive Optical Networks: Common Transmission Convergence Layer Specification, Sept. 2021.
- [7] R. Borkowski et al., "Operator Trial of 100 Gbit/s FLCs-PON Prototype with Probabilistic Shaping and Soft-Input FEC," European Conference on Optical Communication (ECOC), 2021, pp. 1-4.
- [8] R. Matsumoto, K. Matsuda, and N. Suzuki, "Fast, Low-Complexity Widely-Linear Compensation for IQ Imbalance in Burst-Mode 100-Gb/s/λ Coherent TDM-PON," Optical Fiber Communication Conference (OFC) 2018, paper M3B.2.
- [9] R. Koma, M. Fujiwara, J.-I. Kani, K.-I. Suzuki, and A. Otaka, "Burst-Mode Digital Signal Processing That Pre-Calculates FIR Filter Coefficients for Digital Coherent PON Upstream," Journal of Optical Communications and Networking, vol. 10, no. 5, pp. 461–470, May 2018.
- [10] M. Luo, D. Wu, W. Li, T. Zeng, L. Zhou, L. Meng, Z. He, C. Li, and X. Li, "Demonstration of Bidirectional Real-Time 100 Gb/s (4×25 Gb/s) Coherent UDWDM-PON with Power Budget of 44 dB," Optical Fiber Communication Conference (OFC) 2019, paper Th3F.2.
- [11] K. Matsuda, R. Matsumoto, and N. Suzuki, "Hardware-Efficient Adaptive Equalization and Carrier Phase Recovery for 100-Gb/s/λ-Based Coherent WDM-PON Systems," Journal of Lightwave Technology, vol. 36, no. 8, pp. 1492–1497, Apr. 2018.
- [12] J. Zhang, Z. Jia, H. Zhang, M. Xu, J. Zhu and L. A. Campos, "Rate-Flexible Single-Wavelength TFDm 100G Coherent PON Based on Digital Subcarrier Multiplexing Technology," 2020 Optical Fiber Communications Conference and Exhibition (OFC), San Diego, CA, USA, 2020, paper W1E.5.
- [13] D. Welch et al., "Point-to-Multipoint Optical Networks Using Coherent Digital Subcarriers," in Journal of Lightwave Technology, vol. 39, no. 16, pp. 5232-5247, 15 Aug. 15, 2021.
- [14] M. Xu, Z. Jia, H. Zhang, L. A. Campos and C. Knittle, "Intelligent Burst Receiving Control in 100G Coherent PON with 4×25G TFDm Upstream Transmission," 2022 Optical Fiber Communications Conference and Exhibition (OFC), San Diego, CA, USA, 2022, paper Th3E.2.

- [15] H. Zhang, Z. Jia, L. A. Campos and C. Knittle, " Low-Cost 100G Coherent PON Enabled by TFDM Digital Subchannels and Optical Injection Locking," 2023 Optical Fiber Communications Conference and Exhibition (OFC), San Diego, CA, USA, 2023, paper W1I.4.
- [16] J. Zhang, Z. Jia, M. Xu, H. Zhang, L. A. Campos, and C. Knittle, "High-Performance Preamble Design and Upstream Burst-Mode Detection in 100-Gb/s/λ TDM Coherent-PON," Optical Fiber Communication Conference (OFC) 2020, paper W1E.1.
- [17] Z. Y. Choi and Y. H. Lee, "Frame synchronization in the presence of frequency offset," in IEEE Transactions on Communications, vol. 50, no. 7, pp. 1062-1065, July 2002.
- [18] International Telecommunication Union (ITU-T) G.709.2 recommendation.
- [19] Optical Interworking Forum 400G ZR standard.
- [20] T. Duthel, et al, "DSP Design for Point-to-Multipoint Transmission," 2023 Optical Fiber Communications Conference and Exhibition (OFC), San Diego, CA, USA, 2023, paper W1E.1.